Elsevier Editorial System(tm) for Catalysis Today
Manuscript Draft

Manuscript Number: CATTOD-D-14-00403R1

Title: Effect of the metal precursor on the properties of Pt/CeO2/C catalysts for the total oxidation of ethanol

Article Type: SI: Carbocat VI

Keywords: VOCs; ethanol combustion; Toluene hydrogenation; Pt precursor; Ceria; activated carbon.

Corresponding Author: Prof. Antonio Sepúlveda-Escribano, PhD

Corresponding Author's Institution: University of Alicante

First Author: Zinab Abdelouahab-Reddam

Order of Authors: Zinab Abdelouahab-Reddam; Rachad El Mail; Fernando Coloma-Pascual; Antonio Sepúlveda-Escribano, PhD

Manuscript Region of Origin: SPAIN

Abstract: Two series of ceria-promoted carbon-supported platinum catalysts have been prepared and evaluated in total oxidation of ethanol, as a model volatile organic compound (VOC), in order to study the effect of the metal precursor (H2PtCl6 or Pt(NH3)4(NO3)2) on their physico-chemical properties and catalytic behavior. Catalysts with Pt loading of 1 wt.% and ceria loading of 5, 10 and 20 wt.% have been prepared by the impregnation method, and characterized by several techniques (N2 adsorption at 77 K, ICP, XRD, H2-TPR and XPS). Toluene hydrogenation has been used to obtain an estimation of the platinum dispersion on the investigated catalysts. On the other hand, their catalytic behavior has been evaluated in the total oxidation of ethanol, selected as a VOCs probe molecule. A much higher catalytic activity and selectivity to CO2 was achieved with chlorinated catalysts. This behavior has been correlated with a high platinum dispersion and a strong metal-CeO2 interaction in these catalysts which promotes their redox properties.

Highlights

- Highly efficient catalysts for the complete oxidation of ethanol have been developed.

- The use of CeO_2 as promoter is optimized by dispersing it over the activated carbon surface.

- Impact of the platinum precursor (chlorinated or Cl-free) on the catalytic activity.

- $Pt/CeO_2/C$ catalysts are more active than Pt/CeO_2.

Graphical Abstract (for review)

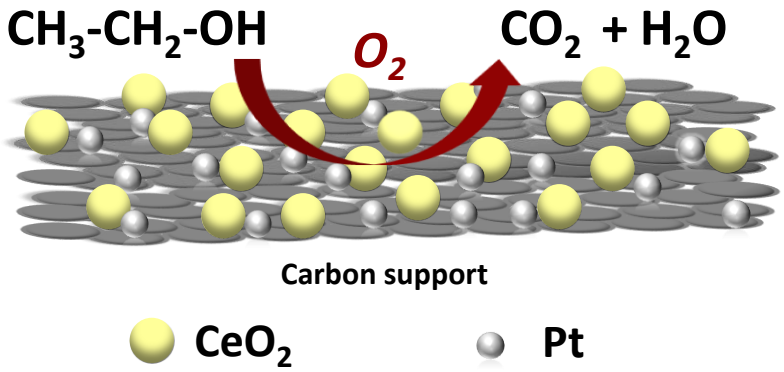

Effect of the metal precursor on the properties of $Pt/CeO_2/C$ catalysts for the total oxidation of ethanol

Z. Abdelouahab-Reddam[1,2], R. El Mail[2], F.Coloma-Pascual[1], A. Sepúlveda-Escribano[1*]

(1) Laboratorio de Materiales Avanzados, Departamento de Química Inorgánica - Instituto Universitario de Materiales de Alicante, Universidad de Alicante, Apartado 99, E-03080, Alicante, Spain
(2) Equipe de Recherche Chimie de l'Eau et Pollution Atmosphérique, Département de Chimie, Faculté des Sciences, Université Abdelmalek Essaadi, Tétouan, Morocco

* Corresponding author: asepul@ua.es ; + 34 965 90 3974

Abstract

Two series of ceria-promoted carbon-supported platinum catalysts have been prepared and evaluated in total oxidation of ethanol, as a model volatile organic compound (VOC), in order to study the effect of the metal precursor (H_2PtCl_6 or $Pt(NH_3)_4(NO_3)_2$) on their physico-chemical properties and catalytic behavior. Catalysts with Pt loading of 1 wt.% and ceria loading of 5, 10 and 20 wt.% have been prepared by the impregnation method, and characterized by several techniques (N_2 adsorption at 77 K, ICP, XRD, H_2-TPR and XPS). Toluene hydrogenation has been used to obtain an estimation of the platinum dispersion on the investigated catalysts. On the other hand, their catalytic behavior has been evaluated in the total oxidation of ethanol, selected as a VOCs probe molecule. A much higher catalytic activity and selectivity to CO_2 was achieved with chlorinated catalysts. This behavior has been correlated with a high platinum dispersion and a strong metal-CeO_2 interaction in these catalysts which promotes their redox properties.

Keywords: VOCs; ethanol combustion; Toluene hydrogenation; Pt precursor; Ceria; activated carbon.

1. INTRODUCTION

Volatile organic compounds (VOCs) are considered a major class of air pollutants because of their harmful effects on human health and the environment. These compounds can cause several health problems which range from minor discomfort to serious medical problems, even some of them are believed to be carcinogenic after prolonged exposure [1,2]. Furthermore, these compounds give rise to the formation of photochemical ozone, which can affect both human health and environment [3]. Among the different techniques available to reduce VOCs emission, catalytic combustion appears to be one of the most efficient [4]. Thus, this technique allows an important reduction of the energy consumption and the formation of undesirable by-products (dioxins and NO_x) by reducing the operating temperature. In general, the catalysts typically used for this application are supported noble metals (Pt, Pd, Rh, Au, etc.,) and metal oxides (CeO_2, CuO, MnO_x, CoO_x, etc.,) [5-10]. Particularly, ceria has been demonstrated to be a promising catalyst in the total oxidation of VOCs, either pure or in combination with noble metals or other metal oxides [11-15]. The high activity of ceria in oxidation reactions is attributed to its high oxygen storage capacity (OSC) and its exceptional redox properties [16]. These features are improved in the presence of noble metals due to its ability to enhance the reducibility of ceria and then their catalytic activity [16-18]. However, ceria presents some disadvantages such as low surface area and relatively high cost, which limit to some extent its use as a bulk unsupported catalyst. In this way, activated carbon seems to be a suitable support for ceria catalyst destined to be used in the complete oxidation of VOCs not only because of its high surface area, but also due to its hydrophobic character. It should be taken into account that the total oxidation of VOCs produces water as one of the final products of the reaction, in addition to the water vapor usually present in the real emissions. In the case of hydrophilic materials, as many of the inorganic oxides are, water molecules are adsorbed on the catalyst surface causing its deactivation, especially when the reaction is performed at low temperatures.

Several studies have investigated the effect of the metal precursor on noble metal catalysts supported on ceria, and they have shown that the nature of the precursor used significantly affects the properties of the catalyst and its catalytic activity in oxidation

reactions. Thus, Bernal *et al.* observed that in Rh/CeO_2 catalysts prepared from chlorinated metal precursor, the presence of residual chlorine ions at the surface of the catalysts changes the redox behavior of ceria. This was explained by the substitution of lattice oxygen ions by the residual chloride ions, forming a highly stable cerium oxychloride at temperatures as low as 573 K, which limits the spillover of hydrogen responsible for the reduction of ceria [19]. On the other hand, Kim *et al.* investigated the effect of the platinum precursor on the activity of Pt/Al_2O_3 catalysts promoted by ceria for the wet oxidation of phenol. The metal was introduced by using two different precursors: anionic (H_2PtCl_6) and cationic ($Pt(NH_3)_4Cl_2$). It was found that the activity of the catalysts depended on the nature of the platinum precursor. Thus, catalysts prepared from the anionic precursor showed much higher activity in the reaction than those prepared from the cationic one. This behavior was attributed to the differences in platinum dispersion and $Pt-CeO_2$ interaction, which seems to be improved in the case of the anionic precursor [20]. In this sense, the aim of the present paper is to prepare platinum catalysts supported on highly dispersed ceria on activated carbon from different platinum precursors, H_2PtCl_6 and $Pt(NH_3)_4(NO_3)_2$, and then to evaluate the effect of the metallic precursor on the physico-chemical properties and the catalytic behavior of these catalysts in total oxidation of ethanol, selected as representative VOC compound.

2. EXPERIMENTAL

2.1. Catalysts preparation

CeO_2/C supports were prepared by impregnation of a commercial activated carbon supplied by Mead Westvaco (Nuchar RGC 30) with acetone solutions containing the appropriate amounts of the precursor ($Ce(NO_3)_3{\cdot}6H_2O$) to obtain ceria loadings of 5, 10 and 20 wt.%. The excess of solvent was removed by flowing nitrogen through the solution at room temperature, and then the samples were dried at 383 K overnight. Finally, the supports were treated under flowing helium (50 $mL{\cdot}min^{-1}$) at 623 K for 5 h, with a heating rate of 1 $K{\cdot}min^{-1}$, in order to decompose the cerium precursor and to obtain CeO_2 [21]. For comparative purposes, a bulk ceria support was prepared by precipitation from an aqueous solution of $Ce(NO_3)_3{\cdot}6H_2O$ containing an excess of urea.

The solution was heated at 353-363 K and kept under stirring during 8 h, in order to facilitate urea decomposition. Then, a few drops of concentrated ammonia solution were added slowly with stirring to ensure complete precipitation. The suspension was then cooled down to room temperature, filtered and washed with ultrapure water. The resulting solid was dried at 383 K for 12 h and finally calcined at 673 K for 4 h, with a heating rate of 3 $K \cdot min^{-1}$.

Pt catalysts were synthesized by the impregnation of the previously prepared ceria/carbon supports with an acetone solution of H_2PtCl_6 or an aqueous solution of $Pt(NH_3)_4(NO_3)_2$. In both cases, the platinum loading was of 1 wt.%. These samples will be referred as, respectively, Pt-Ce/C(Cl) and Pt-Ce/C(N). Following the impregnation process, the solvent excess was removed under vacuum at room temperature and the catalysts were dried overnight at 383 K. Finally, the chlorine-free catalysts were treated at 623 K for 1 h under flowing helium (50 $mL \cdot min^{-1}$), with a heating rate of 1 $K \cdot min^{-1}$, whereas chlorinated catalysts were not submitted to any heat treatment after impregnation.

2.2. Catalysts characterization

The textural properties of the supports have been determined by N_2 adsorption at 77 K on a home-designed and made fully automated manometric equipment. Before any adsorption experiment, samples were out-gassed under UHV conditions (10^{-3} Pa) at 523 K for 4 h. The total pore volume was estimated by the uptake at a relative pressure of 0.95. The micropore volume, V_0, was determined by application of the Dubinin-Radushkevich (DR) equation, while the mesopore volume, V_{meso}, was calculated as the difference between the volume of micropores V_0 and the total pore volume. Specific surface area, S_{BET}, was calculated using the BET equation.

The actual metal loading of the different catalysts was determined by ICP-OES analysis in a Perkin-Elmer 7300DV spectrometer.

The X-ray diffraction patterns of the catalysts were recorded on a JSO-Debyeflex 2002 system, from Seifert, fitted with a Cu cathode and a Ni filter, using a $20^{o}.min^{-1}$ scanning

rate. The average crystal size for CeO_2 was estimated by application of the Scherrer equation to the (111) ceria diffraction peak.

Temperature-programmed reduction (TPR) measurements were carried out in a U-shaped quartz reactor, using a 5%H_2/He gas flow of 50 mL·min^{-1} and about 100 mg of catalyst. The temperature was raised at 10 K·min^{-1} from room temperature to 1273 K. Hydrogen consumption was followed by online mass spectrometry.

X-ray photoelectron spectroscopy (XPS) was performed with a K-ALPHA, Thermo Scientific spectrometer, using Al-K radiation (1486.6 eV), monochromatized by a twin crystal monochromator and yielding a focused X-ray spot with a diameter of 400 µm, at 3 mA × 12 kV. The alpha hemispherical analyser was operated in the constant energy mode with survey scan pass energies of 200 eV to measure the whole energy band and 50 eV in a narrow scan to selectively measure the particular elements. Charge compensation was achieved with the system flood gun that provides low energy electrons and low energy argon ions from a single source. The quantitative analysis were estimated by calculating the integral of each peak after subtracting the S-shaped background and fitting the experimental curve to a combination of Lorentzian (30%) and Gaussian (70%) lines. Reduction of the samples were carried out "ex situ" in an U-shaped quartz reactor under flowing hydrogen (50 ml.min^{-1}) at 473 K for 1h and introduced in an octane solution (in inert atmosphere). Suspensions were evaporated in the XPS system under vacuum conditions.

2.3. Catalytic tests

The catalytic behaviour of the prepared catalysts was investigated in two different reactions, toluene hydrogenation and the complete combustion of ethanol.

Toluene hydrogenation was carried out in a U-shape quartz reactor at atmospheric pressure using 100 mg of catalyst diluted in SiC to a total volume of 1.5 ml. Prior to starting the reaction, all the samples were reduced in situ at 473 and 773 K (2 K·min^{-1}) for 2 h under hydrogen flow (50 mL·min^{-1}) and then cooled under H_2 to reaction temperature (333 K). Then, the catalyst were contacted with a reactant mixture of a total flow of 50 mL·min^{-1} containing hydrogen and toluene in a H_2/C_7H_8 ratio of 36 prepared

by passing the hydrogen flow through a thermostabilized saturator containing toluene at 293 K. The concentrations of the reactants and the products were determined using an on-line gas chromatograph (Agilent 6890N) equipped with a flame ionization detector and HP-Plot/Q (30 m x 0.53 mm) column.

Ethanol oxidation experiments were carried out in a U-shape quartz reactor, operating in continuous mode, using 150 mg of catalyst diluted in SiC to a total volume of 1.5 mL. Prior to reaction, the catalysts was reduced in situ under flowing hydrogen (50 $mL \cdot min^{-1}$) at 473 K for 1 h (2 $K \cdot min^{-1}$). Then, H_2 was replaced by He at the same temperature during 1 h and the catalyst was cooled to temperature reaction under He flow. The reaction mixture containing 1000 ppm of ethanol in air flow of 100 $mL \cdot min^{-1}$ was prepared by passing air flow through a thermostabilized saturator containing ethanol. The catalytic activity was evaluated in the temperature range 323-473 K under atmospheric pressure. Reaction products were analyzed by on-line gas chromatography (Agilent 6890N) equipped with a flame ionization detector and HP-Plot/Q (30 m x 0.53 mm) column. An on-line IR detector (SENSOTRAN IR) was also employed for the quantitative analysis of CO_2. In humid condition, distilled water was injected by a Gilson 307 HPLC pump and evaporated in a heat box, operating at 473 K. All gas lines of the reaction system were heated to 383 K in order to avoid ethanol and water adsorption and condensation on tube walls.

3. RESULTS AND DISCUSSION

3.1. Characterization

3.1.1. N_2 adsorption

All the N_2 adsorption-desorption isotherms (not shown) for the original activated carbon and the ceria-containing supports correspond to a mixed Type I and IV isotherms. These isotherms are characterized by a large adsorption capacity at low relative pressures, characteristic of microporous materials, and a hysteresis loop at high relative pressures, which indicates the presence of a certain proportion of mesoporosity. The textural properties obtained from the isotherms of the different supports are summarized in

Table 1. As it can be seen, both the BET surface area and the total pore volume decrease with increasing the ceria loading. This reduction could be due to a partial blockage of the activated carbon porosity by the ceria crystallites. Furthermore, it should be taken into account that the loss of carbon mass in the sample after the introduction of ceria contributes to the reduction of the porosity because the ceria provides lower surface area than the same mass of activated carbon, as can be seen in Table 1. On the other hand, loading of Pt did not affect the porous texture of the supports and, thus, the textural parameters of the catalysts were similar to those of the supports.

3.1.2. ICP-OES

Table 2 shows the metal loading of the prepared catalysts determined by ICP-OES. The Pt loading obtained is in good agreement with the nominal one of 1 wt.% for all the catalysts except for $Pt/CeO_2(N)$, for which a slightly lower platinum content is found (0.66 wt.%). However, the actual ceria loading is lower than the nominal values for all the samples, which may be due to the fact that not all the amount of ceria employed during the preparation was actually incorporated in the catalysts.

3.1.3. X-ray diffraction

XRD patterns for the prepared catalysts are shown in Fig. 1. All the profiles show four diffraction peaks, at 28.5º, 33º, 47.5º and 56.3º, characteristic of the fluorite phase of ceria (JCPDS 34-394). The supported catalysts show broader peaks compared with the unsupported Pt/CeO_2, which indicates a high dispersion of ceria particles on the carbonaceous support. On the other hand, the intensity of the peaks of the supported catalysts increases as the ceria loading increases. However, the diffraction peaks of the catalysts prepared from $((NH_3)_4Pt(NO_3)_2)$ are somewhat more defined and intense with respect to their counterparts prepared from the chlorinated precursor. This suggests that a slight alteration of the support has taken place during the impregnation with the chlorinated platinum precursor, since the catalysts with the same ceria loading have been prepared from the same support. The comparison of the X-ray diffraction patterns of the catalysts with those of their corresponding supports (not shown) reveals a great

similarity between the latest and the diffractograms of the chlorine-free catalysts. These results confirm that a structural modification of ceria has taken place during the impregnation with the chlorinated platinum precursor, what could be related to the residual chlorine originated from H_2PtCl_6. Table 2 summarizes the average crystallite size of ceria calculated by the Scherrer equation. It can be clearly seen that the ceria particle size in the unsupported catalysts prepared from both precursors is much larger than in the activated carbon supported catalysts. Finally, no peaks corresponding to platinum can be observed in the XRD patterns of catalysts, this suggesting the presence of very small metal particles.

3.1.4. Temperature-programmed reduction (TPR)

Fig. 2 shows the evolution of H_2 consumption as a function of temperature for the ex-chloride and ex-nitrate catalysts. The chlorinated unsupported catalyst exhibits three reduction processes, approximately at 518, 730 and 924 K. The peak at low temperature is commonly associated to the surface reduction of ceria in close contact with the metal as well as the reduction of platinum species. The second peak at 730 K can be attributed to the surface reduction of ceria which is not in close contact with the platinum particles, whereas the broad peak at high temperatures corresponds to the bulk reduction of ceria [22-24]. The TPR profiles of the chlorinated supported catalysts display similar features to $Pt/CeO_2(Cl)$, with two overlapping peaks in the temperature range from 355 to 600 K and a broad shoulder centered approximately at 845 K. Thus, similar assignments are made for them. The peak shift toward lower temperatures in the reduction profiles of the supported catalysts with respect to the bulk catalyst confirms the presence of small particles of ceria highly dispersed on the carbonaceous support surface, which makes its reduction easier than in the bulk catalyst. Furthermore, the appearance of these peaks at low temperatures indicates that the ceria particles are in intimate contact with the metal, which promotes the reduction of the oxide at lower temperatures by hydrogen spillover from the metal to the support.

The chlorine-free catalysts exhibit different profiles than those of the chlorinated ones. $Pt/CeO_2(N)$ shows, as $Pt/CeO_2(Cl)$, three processes of hydrogen consumption. However, the first reduction peak is considerably less intense and appears at lower temperatures

with respect to the catalyst prepared with H_2PtCl_6. This peak is assigned, as already has been mentioned, to the surface reduction of ceria in close contact with metal, as well as the reduction of the Pt–O–CeO_2 oxidized species formed upon samples heat treatment. The region at high temperatures (from 780 K) consists of two broad bands which could be attributed to the bulk reduction of ceria, while the reduction process between 470 and 700 K may be associated with the reduction of ceria species with less contact with the metal and which interacts with it to different extents [16,24]. Moreover, despite the great similarity between the TPR profiles of Pt/CeO_2(N) and the supported catalysts prepared from the same precursor, these latter are mainly characterized by the absence of the hydrogen consumption peak at low temperature originated by the surface reduction of ceria particles in intimate contact with the metal. The absence of this peak in these catalysts, together with its low intensity in the TPR profile of the bulk catalyst, could suggest that the metal-ceria interaction in these samples is weak. However, this interaction seems to be stronger in the case of the chlorinated catalysts. On the other hand, the appearance of broad shoulders as multiple overlapping peaks in the reduction profiles of the ex-nitrate catalysts indicates the surface heterogeneity [24-26].

It can be seen that, in spite of the weak metal-oxide interaction in the ex-nitrate catalysts, the first reduction process for the Pt/CeO_2(N) catalyst begins at lower temperature compared with its chlorinated counterpart. This behavior might be explained by an inhibiting effect of residual chloride ions on the reducibility of ceria in Pt/CeO_2(Cl) catalyst. This effect has been widely described in the literature for different systems M/CeO_2 prepared from chlorinated metal precursors. In this sense, several studies on platinum supported on ceria catalyst prepared from a chlorinated precursor report that the presence of residual chlorine in such catalysts inhibits the platinum reduction due to the formation of stable oxychloroplatinum species (PtO_xCl_y), whose reduction requires higher temperatures compared to PtO_x species [27-30]. Furthermore, it has been demonstrated that the residual chlorine ions are mobile, and they can diffuse on the ceria support during the reduction treatment and replace surface O^{2-} ions to form CeOCl. The formation of these species on the oxide surface inhibits both the direct and back spillover process of hydrogen responsible for the reducibility of the superficial ceria [19,31-37].

3.1.5. X-ray photoelectron spectroscopy (XPS)

Fig. 3 illustrates the Pt 4f XPS spectra of Pt-10Ce/C(Cl) and Pt-10Ce/C(N), both fresh and reduced at 473 K. All the spectra consist of two broad bands, corresponding to the Pt $4f_{7/2}$ and Pt $4f_{5/2}$ levels, which have been deconvoluted into two contributions. The binding energies of each component of Pt $4f_{7/2}$ level and its contribution on the main band are reported in Table 3. The as-prepared Pt-10Ce/C(Cl) catalyst exhibits two peaks at 72.6 and 73.9 eV which, according to the literature, can be assigned, respectively, to Pt(II) and Pt(IV) species [38,39]. The reduction treatment at 473 K produces a shift of these contributions to lower binding energy, showing two peaks at 71.5 and 73.3 eV. The first one could be attributed to metallic platinum, while the other one corresponds to platinum species in oxidized state [25]. For the fresh ex-nitrate catalyst, two peaks at 71.8 and 72.9 eV corresponding to metallic platinum and Pt(II) species, respectively, have been observed. The reduction treatment does not change the energy values of the Pt 4f bands for this catalyst, but it leads to a significant difference in the distribution of components. Concretely, the proportion corresponding to the peak at low energy increases from 33.3% to 73.5%, indicating the presence of a higher amount of reduced platinum [40]. Thus, the reduction treatment at 473 K achieves only the reduction of about half of the platinum present in the chlorinated catalyst. In contrast, in its counterpart chlorine-free catalyst, a significant amount of platinum is already in the metallic state in the fresh catalyst without any reduction treatment. This behavior is in accordance with the TPR results discussed above. Thus, the more difficult reduction of platinum in the chlorinated catalyst could be due to the strong interaction between the metal and the ceria particles, which hinders the reduction of the metal at lower temperature. Besides, the presence of residual chlorine inhibits the platinum reduction through the formation of stable oxychloroplatinum species. However, the same treatment reduces the majority of the platinum on the surface of Pt-10Ce/C(N) catalyst. This can be explained by the very weak interaction Pt–CeO_2 in the ex-nitrate catalyst, which is clearly confirmed by the absence of the peak at lower temperature in the TPR profiles.

The percentages of reduced Ce(III) and the Pt/Ce, Ce/C and Cl/C atomic ratios for the fresh and reduced Pt-10Ce/C(Cl) and Pt-10Ce/C(N) catalysts are reported in Table 3. The degree of ceria reduction was estimated using the following equation [41-43]:

$$\%Ce(III) = \frac{[S(u_0) + S(u') + S(v_0) + S(v')]}{\sum[S(u) + S(v)]} \times 100$$

where u and v are the peaks corresponding to the components of $3d_{5/2}$ and $3d_{3/2}$, respectively, according with the nomenclature of Burroughs [44-48].

As it can be seen, the reduction treatment at 473 K produces a slight decrease in the Pt/Ce atomic ratio for the chlorinated catalyst, indicating a very slight sintering of the platinum particles. In contrast, this decrease is very important in the case of chlorine-free catalyst, what confirms the absence of an intimate interaction between the platinum and the ceria oxide that may inhibit the sintering of metallic particles. The Ce/C atomic ratio does not change for any of the catalysts after the reduction at 473 K, this indicating that this treatment does not alter the dispersion of the ceria particles.

On the other hand, it can be observed that in both catalysts there is a significant amount of Ce(III) even before the reduction treatment. This amount is practically the same for both samples and can be due, probably, to a photoreduction process of ceria during XPS experiment [42,43,46,47]. Nevertheless, the reduction treatment at 473 K leads to different behavior in the catalysts. Indeed, while this treatment has no significant effect on the chlorine-free catalyst, the Ce(III) proportion increases from 43.3% to 51.3% in the case of its chlorinated counterpart. This behavior has been reported in previous studies and it has been attributed to the formation of surface CeOCl species, in which cerium ions have been reduced from Ce(IV) to Ce(III). Moreover, the increase of the Cl/Ce atomic ratio after reduction at 473 K from 0.3 to 0.5 confirms the chlorine surface enrichment of the catalyst during the reduction treatment, which may be related to the formation of surface CeOCl crystallites [19,25,35].

On the other hand, these results are in good agreement with those obtained by TPR and confirm that there is an intimate interaction between the metal and the ceria particles in the ex-chloride catalysts, which promotes the reduction of the oxide by H_2 spillover at relatively low temperatures. However, this interaction seems to be very weak in the chlorine-free catalysts.

3.2. Catalytic activity

3.2.1. Toluene hydrogenation

Toluene hydrogenation has been employed to obtain an estimation of the platinum dispersion in the investigated catalysts. It is well know that chemisorption measurements, which are commonly used to determine the metallic dispersion, is not viable in the case of metallic catalysts containing ceria, given that the latter can chemisorb both H_2 and CO at room temperature [49-51], this causing an overestimation of the amount of surface metal exposed [52,53]. Therefore, the use of a structure-insensitive reaction, such as toluene hydrogenation, can be a good alternative to evaluate the metallic dispersion in ceria-containing catalysts. The catalytic activity in toluene hydrogenation only depends on the amount of metal available at the catalyst surface, regardless of the support structure and the metal particle size or crystallographic plane. However, the structure-insensitive character of the reaction can be affected by the presence of electronic and/or geometrical effect originated on noble metal particles by partially reduced ceria generated after reduction treatments at high temperature, although this effect can be manifested also in the chemisorption process [40]. In this way, toluene hydrogenation has been employed in this study just to obtain the estimation of relative platinum dispersion in the prepared catalysts.

Table 4 reports the catalytic activity for toluene hydrogenation for all the catalysts after reduction at 473 and 773 K. It is worth to mention that the only product of the reaction was methylcyclohexane. Taking into account the lowest reduction temperature, it can be clearly observed that the chlorinated catalysts show higher activity than their chlorine-free counterparts. Furthermore, the hydrogenation activity of the catalysts decreases with increasing the ceria loading independently of the platinum precursor except in the case of Pt-10Ce/C(Cl) catalyst. This latter exhibits the best performance in this reaction, reaching a much higher activity than all the other catalysts (137.8 $\mu mol \cdot s^{-1} \cdot gPt^{-1}$). As mentioned before, the activity in this reaction depends exclusively on the amount of metal exposed on the surface of the catalyst. Furthermore, the strong metal-support interaction effect due to the partially reduced ceria particles is not expected after reduction at low temperature (473 K). So, it can be deduced that the highest activity

exhibited by the chlorinated catalysts is related to a higher metallic dispersion in these catalysts compared with the ex-nitrate catalysts, and that the chlorinated Pt-10Ce/C catalyst presents the highest Pt dispersion. Moreover, the obtained results show that the degree of platinum dispersion on the chlorine-free catalysts is low. This behavior could be explained in terms of the mechanism of the platinum adsorption. Thus, ceria particles exhibit positive surface charge when suspended in aqueous solution, which causes an electrostatic repulsion between $Pt(NH_3)_4^{2+}$ platinum cation and ceria because of their charges of the same sign. This repulsion inhibits the adsorption of the platinum cation on ceria, resulting in large metal particles. This could also explain why platinum dispersion decreases when increases the amount of ceria in these catalysts and why platinum and ceria particles are not in close contact in the ex-nitrate catalysts.

On the other hand, the increase in the reduction temperature of 473 to 773 K produces a very strong decrease of the activity values of all the catalysts, obtaining very low or almost null values after reduction at 773 K. However, this deactivation is more important in the case of chlorinated catalysts. This deactivation has been observed in several studies on noble metal catalysts supported on ceria in the reaction of toluene and benzene after reduction at high temperature, and it has been explained by the presence of a strong interaction between the metal and the ceria particles generated by the reduction at high temperature, or by the sintering of the platinum particles after the reduction treatment, although several studies discarded this possibility on the basis of XPS results [24,40,54-58]. In the case of chlorinated catalysts, TPR and XPS results confirm the presence of a close contact with platinum a ceria, which prevents the sintering of metal particles. So, the deactivation observed for the chlorinated catalysts could be related to a strong metal support interaction induced upon reduction at high temperature. Regarding the chlorine-free catalysts, the decrease in the hydrogenation activity after reduction at 773 K might be explained by the presence of electronic effects between platinum and ceria as in the case of the chlorinated catalyst. However, the deactivation of these catalysts should be mainly due to the sintering of Pt particles during the reduction at high temperature, given the absence of an intimate interaction between ceria and platinum which may inhibit sintering of the metal particles after reduction at 773 K. Indeed, XPS results show sintering platinum particles on Pt-10Ce/C(N) catalyst even after reduction at lower temperature (473 K).

3.2.2. Total oxidation of ethanol

Fig. 4 illustrates the evolution of the ethanol conversion as a function of reaction temperature on the chlorinated and chlorine-free catalysts. For the aim of comparison, the conversion profiles of 10Ce/C and bulk ceria CeO_2 supports have also been included in the Figure. The reaction products in all cases were acetaldehyde, CO_2 and water. It can be clearly seen that the chlorinated catalysts show a higher conversion than chlorine-free ones, achieving the total conversion of ethanol at lower temperatures. Nevertheless, the prepared catalysts exhibit a similar trend in the studied temperature range regardless of the metallic precursor. Thus, at low temperatures the activity of the catalysts decreases with increasing the ceria loading, while at relatively high temperatures the order of the activity observed is: Pt-10Ce/C>Pt-20Ce/C>Pt-5Ce/C>Pt/CeO_2 for both series. This behavior has been observed in previous studies and seems to indicate that there are two different reaction mechanisms, at high and low temperature [59]. The catalyst with 10 wt.% ceria shows the highest conversion of ethanol independently of the platinum precursor, achieving a complete conversion of ethanol at 398 and 448 K with the chlorinated and the chlorine-free catalyst, respectively. Furthermore, the bulk catalysts prepared from both precursors show much lower conversion than the carbon-supported catalysts.

The evolution of the CO_2 yield as a function of the reaction temperature for all the catalysts, and also for the 10Ce/C and bulk ceria CeO_2 supports, is shown in Fig. 5. Over the whole temperature range, the chlorinated and ex-nitrate catalysts show the same trend, obtaining the following order in selectivity: Pt-10Ce/C>Pt-20Ce/C>Pt-5Ce/C>Pt/CeO_2. The optimum catalyst prepared with the chlorinated precursor reaches a total conversion of ethanol to CO_2 at 433 k, whereas its chlorine-free counterpart achieves the same conversion at a higher temperature (473 K). On the other hand, the catalysts with the bulk ceria support (Pt/CeO_2(Cl) and Pt/CeO_2(N)) exhibit low selectivity in comparison with the carbon-supported catalysts, in such a way that they convert only 66 and 56% of ethanol to CO_2, respectively, at 473 K. Furthermore, it can be seen that the supports exhibit a much lower activity than the corresponding catalysts, both the chlorinated and the chlorine-free ones. This expected behavior is attributed to

the ability of platinum to facilitate the reducibility of ceria at low temperatures and thus improve its catalytic activity in the total oxidation of ethanol.

The results obtained for ethanol oxidation are consistent with those obtained for toluene hydrogenation, that indicate that the higher activity of ex-chloride catalysts in the total oxidation of ethanol compared with the chlorine-free counterparts is due in part to the high dispersion of platinum. In addition, the higher activity exhibited by these catalysts, despite the presence of residual chlorine which is undesirable for the reaction, should be mainly related to the presence of an intimate interaction between the ceria and the highly dispersed platinum particles. Indeed, the interaction between the metal and the oxide is an important factor in catalytic oxidation reactions over noble metal catalysts supported on ceria. This interaction promotes the generation of highly active sites at the Pt−CeO_2 interface, because the metal improves the redox properties of ceria and therefore enhances the activity/mobility of lattice oxygen, which participates in the reaction through a Mars-van Krevelen mechanism [60-62]. Likewise, the behavior of Pt-10Ce/C(Cl), which shows the best performance in terms of both activity and selectivity in the complete oxidation of ethanol, could be due to an optimal Pt−CeO_2 interaction, favored by the presence of an optimal ceria loading along with a high dispersion of metal as evidenced by the results of the hydrogenation reaction.

It is worth mentioning that all the supported catalysts show good activity in the total oxidation of ethanol independently of the metal precursor, achieving higher conversions and selectivities than the bulk ceria-supported catalysts, Pt/CeO_2(Cl) and Pt/CeO_2(N). This behavior is due to the high dispersion of ceria particles on the carbonaceous support, which provides a high active surface and also promotes the Pt−CeO_2 interaction, responsible for the catalytic activity in the investigated reaction.

4. CONCLUSIONS

The preparation of Pt catalysts supported on ceria dispersed on activated carbon using different platinum precursors, H_2PtCl_6 and $Pt(NH_3)_4(NO_3)_2$, leads to catalysts with different properties and catalytic activity in the total oxidation of ethanol. Thus,

characterization results revealed that there is a strong interaction between platinum and ceria particles in the chlorinated catalysts, while this interaction is very weak in their counterparts prepared from the chlorine-free precursor. Moreover, ex-chloride catalysts exhibit higher activity in toluene hydrogenation, indicating a higher dispersion of Pt on these catalysts. In general, the chlorine-free catalysts showed a low hydrogenation activity, which indicates that the degree of platinum dispersion is low. This behavior has been explained in terms of the mechanism of the deposition of the platinum precursor on the catalysts surface, which results in large metal particles with a weak interaction with the ceria nanocrystals. In the total oxidation of ethanol, a much higher catalytic activity and selectivity to CO_2 was achieved with the chlorinated catalysts. This may be due to the high platinum dispersion and the intimate Pt-CeO_2 interaction in these catalysts which promotes their redox properties.

Acknowledgements

Financial support from Generalitat Valenciana (Spain, PROMETEO/2009/002-FEDER and PROMETEOII/2014/004-FEDER) is gratefully acknowledged.

5. REFERENCES

[1] D.W.M. Sin, Y.C. Wong, P.K.K. Louis, Atm. Environ. 35 (2001) 5961-5969.

[2] A.J. Kean, E. Grosjean, D. Grosjean, R.A. Harley, Environ. Sci. Technol. 35 (2001) 4198-4204.

[3] Q. Wang, Z. Han, T. Wang and R. Zhang, Sci Total Environ. 395 (2008) 41-49

[4] L.F. Liotta, Appl. Catal. B: Environ. 100 (2010) 403-412.

[5] S. Scirè, L.F. Liotta, Appl. Catal. B: Environ. 125 (2012) 222- 246.

[6] T. Garcia, B. Solsona, D. Cazorla-Amorós, A. Linares-Solano, S.H. Taylor, Appl. Catal. B: Envrion. 62 (2006) 66-76.

[7] L.M. Petkovic, S.N. Rashkeev, D.M. Ginosar, Catal. Today 147 (2009) 107-114.

[8] H.L. Tidahy, S. Siffert, F. Wyrwalski, J.F. Lamonier, A. Aboukaïs, Catal. Today 119 (2007) 317-320.

[9] F.N. Aguero, A. Scian, B.P. Barbero, L.E. Cadús, Catal. Today 133-135 (2008) 493-501.

[10] B. de Rivas, R. López-Fonseca, C. Jiménez-González, J.I. Gutiérrez-Ortiz, J. Catal. 281 (2011) 88-97.

[11] L. He, Y. Yu, C. Zhang, H. He, J. Environ. Sci. 23 (2011) 160-165.

[12] S. Scirè, P.M. Riccobene, C. Crisafulli, Appl. Catal. B: Environ. 101 (2010) 109-117.

[13] S.S.T. Bastos, S.A.C. Carabineiro, J.J.M. Órfão, M.F.R. Pereira, J.J. Delgado, J.L. Figueiredo, Catal. Today 180 (2012) 148-154.

[14] D. Yu, Y. Liu, Z. Wu, Catal. Commun. 11 (2010) 788-791.

[15] D. Delimaris, T. Ioannides, Appl. Catal. B: Environ. 89 (2009) 295-302.

[16] A. Trovarelli, Catal. Rev. Sci. Eng. 38 (1996) 439-520.

[17] A. Trovarelli, C. De Leitenburg, M. Boaro, G. Dolcetti, Catal. Today 50 (1999) 353-367.

[18] L. Pino, A. Vita, M. Cordaro, V. Recupero, M.S. Hegde, Appl. Catal. A: Gen. 243 (2003) 135-146.

[19] S. Bernal, J.J. Calvino, G.A. Cifredo, J.M. Gatica, J.A. Pérez Omil, A. Laachir, V. Perrichon, Stud. Surf. Sci. Catal. 96 (1995) 419-429.

[20] S-K. Kim, S-K. Ihm, Ind. Eng. Chem. Res. 41 (2002) 1967-1972.

[21] A. Sepúlveda-Escribano, J. Silvestre-Albero, F. Coloma, F. Rodríguez-Reinoso, Stud. Surf. Sci. Catal. 130 (2000) 1013-1018.

[22] H.C Yao, Y.F.Y. Yao, J. Catal. 86 (1984) 254.

[23] F. Fally, V. Perrichon, H. Vidal, J. Kaspar, G. Blanco, J.M. Pintado, S. Bernal, G. Colon, M. Daturi, J.C. Lavalley, Catal. Today 59 (2000) 373-386.

[24] A. Sepúlveda-Escribano, F. Coloma, F. Rodríguez-Reinoso, J. Catal. 178 (1998) 649-657.

[25] J. Silvestre-Albero, F. Coloma, A. Sepúlveda-Escribano, F. Rodríguez-Reinoso, Appl. Catal. A: Gen. 304 (2006) 159-167.

[26] P. Fornasiero, R. Di Monte, G.R. Rao, J. Kaspar, S. Meriani, A. Trovarelli, M. Graziani, J. Catal. 151 (1995) 168-177.

[27] M. Paulis, H. Peyrard, M. Montes, J. Catal. 199 (2001) 30-40.

[28] H. Lieske, G. Lietz, H. Spindler, J. Völter, J. Catal. 81 (1983) 8-16.

[29] E. Marceau, M. Che, J. Saint-Just, J.M. Tatibouët, Catal. Today 29 (1996) 415-419.

[30] C. Contescu, D. Macovei, C. Craiu, C. Teodorescu, J.A. Schwarz, Langmuir 11 (1996) 2031-2040.

[31] F.J. Gracia, J.T. Miller, A.J. Kropf, E.E.Wolf, J. Catal. 209 (2002) 341-354.

[32] F.L. Normand, L. Hilaire, K. Kili, G. Krill, G. Maire, J. Phys. Chem. 92 (1988) 2561-2568.

[33] L. Kępiński, M. Wo□ cyrz, J. Okal, J. Chem. Soc., Faraday Trans. 91 (1995) 507-515.

[34] L. Kępiński, J. Okal, J. Catal. 192 (2000) 48-53.

[35] S. Salasc, V. Perrichon, M. Primet, M. Chevrier, F. Mathis, N. Moral, Catal. Today 50 (1999) 227-235.

[36] C. Force, J.P. Belzunegui, J. Sanz, A. Martínez-Arias, J. Soria, J. Catal. 197 (2001) 192-199.

[37] A. Bensalem, F. Bozon-Verduraz, V. Perrichon, J. Chem. Soc. Faraday Trans. 91 (1995) 2185-2189.

[38] A. Huidobro, A. Sepúlveda-Escribano, F. Rodríguez-Reinoso, J. Catal. 212 (2002) 94-103.

[39] P. Bera, K.R. Priolkar, A. Gayen, P.R. Sarode, M.S. Hegde, S. Emura, R. Kumashiro, V. Jayaram, G.N. Subbanna, Chem. Mater. 15 (2003) 2049-2060.

[40] J. Silvestre-Albero, F. Rodríguez-Reinoso, Sepúlveda-Escribano, J. Catal. 210 (2002) 127-136.

[41] A. Laachir, V. Perrichon, A. Badri, J. Lamotte, E. Catherine, J.C. Lavalley, J. El Fallah, L. Hilaire, F. Le Normand, E. Quéméré, G.N. Sauvion, O. Touret, J. Chem. Soc., Faraday Trans. 87 (1991) 1601-1609.

[42] M. Daturi, C. Binet, J.C Lavalley, A. Galtayries, R. Sporken, Phys. Chem. Chem Phys. 1(1999) 5717-5724.

[43] G. Dong, J. Wang, Y. Gao, S. Chen, Catal. Lett. 58 (1999) 37-41.

[44] P. Burroughs, A. Hammett, A.F. Orchard, G.J. Thornton, J. Chem Soc. Dalton Trans. 17 (1976) 1686-1698.

[45] M. Romeo, K. Bak, J. El Fallah, F. Le Normand, L. Hilaire, Surf. Interf. Anal. 20 (1993) 508-512.

[46] M.S.P. Francisco, V.R. Mastelaro, P.A.P. Nascente, A.O. Florentino, J. Phys. Chem. B 105 (2001) 10515-10522.

[47] J.Z. Shyu, W.H. Weber, H.S. Gandhi, J. Phys. Chem. 92 (1988) 4964-4970.

[48] N. Thromat, M. Gautier-Soyer, G. Bordier, Surf. Sci. (1996) 290-302.

[49] V. Perrichon, L. Retailleau, P. Bazin, M. Daturi, J.C. Lavalley, Appl. Catal. A: Gen. 260 (2004) 1-8.

[50] S. Bernal, J.J. Calvino, G.A. Cifredo, J.M. Gatica, J.A. Pérez Omil, J.M. Pintado, J. Chem. Soc., Faraday Trans. 89 (1993) 3499-3505.

[51] J.L.G. Fierro, J. Soria, J. Solid State Chem. 66 (1987) 154-162.

[52] S. Bernal, J.J. Calvino, G.A. Cifredo, J.M. Rodríguez-Izquierdo, V. Perrichon, A. Laachir, J. Chem. Soc., Chem. Commun. (1992) 460-462.

[53] S. Bernal, J.J. Calvino, G.A. Cifredo, J.M. Rodríguez-Izquierdo, V. Perrichon, A. Laachir, J. Catal. 137 (1992) 1-11.

[54] S. Bernal, F.J. Botana, J.J. Calvino, M.A. Cauqui, G.A. Cifredo, A. Jobacho, J.M. Pintado, J.M. Rodríguez-Izquierdo, J. Phys. Chem. 97 (1993) 4118-4123.

[55] L. Kępiński, M. Wo□ cyrz, J. Okal, J. Chem. Soc., Faraday Trans. 91 (1995) 507-515.

[56] P.N.Da Silva, M. Guenin, C. Leclercq, R. Frety, Appl. Catal. 54 (1989) 203-215.

[57] P. Meriaudeau, J.F. Dutel, M. Dufaux, C. Naccache, Stud. Surf. Sci. Catal. 11 (1982) 95-104.

[58] J.C. Serrano-Ruiz, J. Luettich, A. Sepúlveda-Escribano, F. Rodríguez-Reinoso, J. Catal. 241 (2006) 45-55.

[59] Z. Abbasi, M. Haghighi, E. Fatehifar, S. Saedy., J. Hazard. Mater. 186 (2011) 1445-1454.

[60] M.A. Centeno, M. Paulis, M. Montes, J.A. Odriozola, Appl. Catal. A: Gen. 234 (2002) 65-78.

[61] P. Bera, K.C. Patil, V. Jayaram, G.N. Subbanna, M.S. Hegde, J. Catal. 196 (2000) 293-301.

[62] S. Scirè, S. Minicò, C. Crisafulli, C. Satriano, A. Pistone, Appl. Catal. B: Environ. 40 (2003) 43-49.

Figure

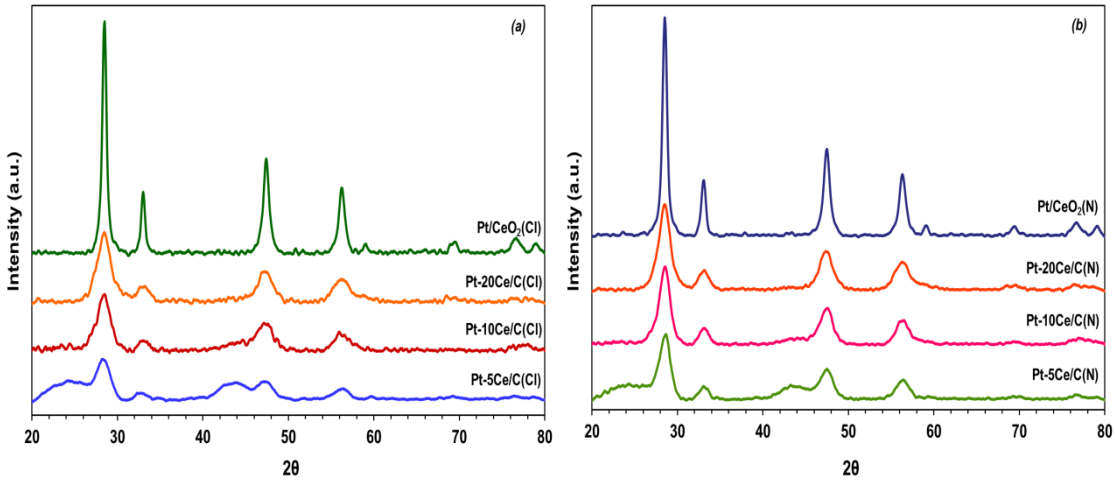

Fig. 1. X-ray diffraction patterns of chlorinated (a) and chlorine-free catalysts (b).

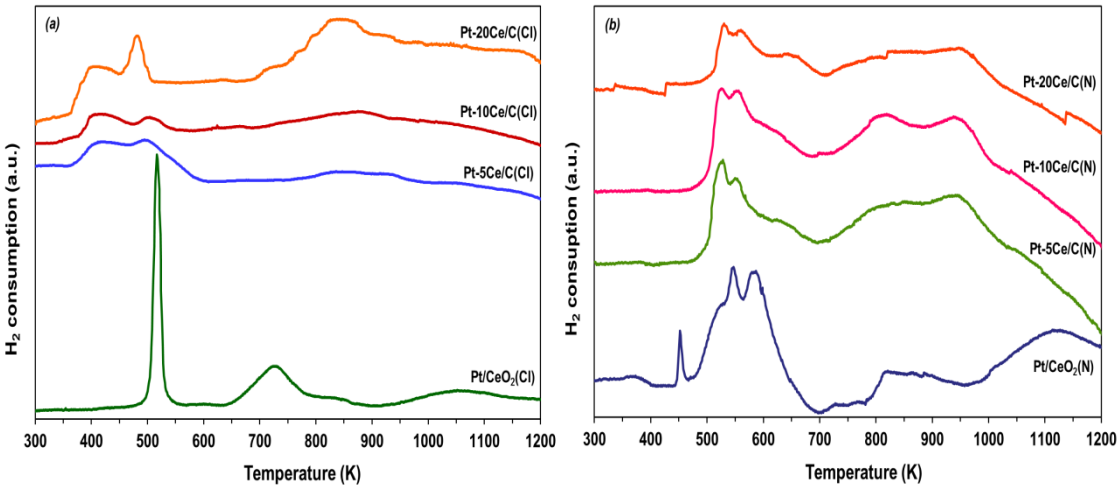

Fig. 2. TPR profiles of the chlorinated (a) and chlorine-free catalysts (b).

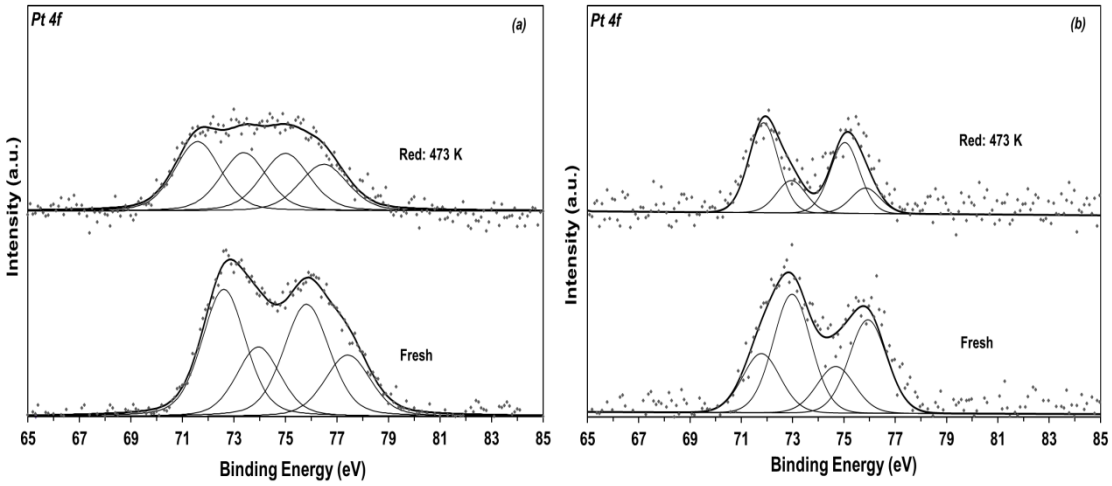

Fig. 3. XPS Pt 4f spectra of the fresh and reduced catalysts at 473 K.
(a)Pt-10Ce/C(Cl); (b) Pt-10Ce/C(N).

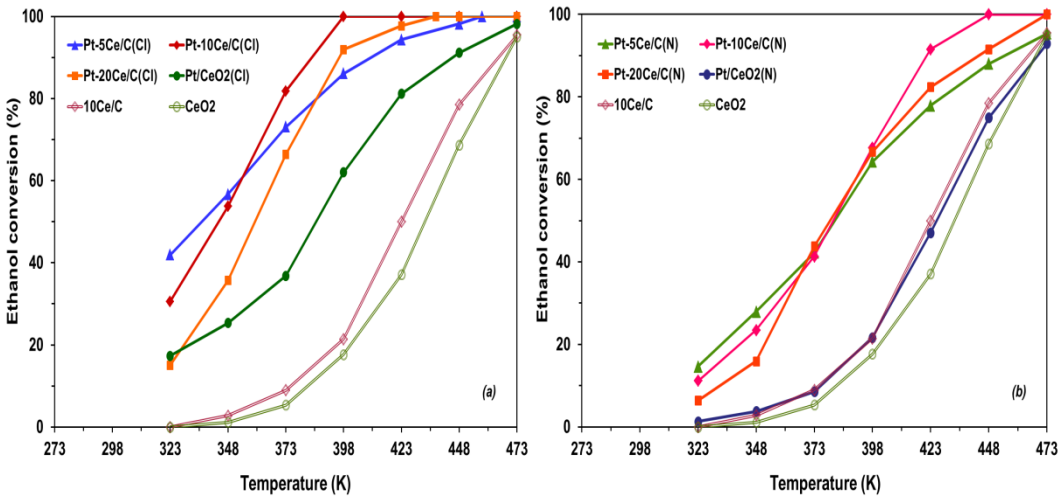

Fig. 4. Ethanol conversion as a function of reaction temperature for ex-chloride (a) and ex-nitrate (b) catalysts.

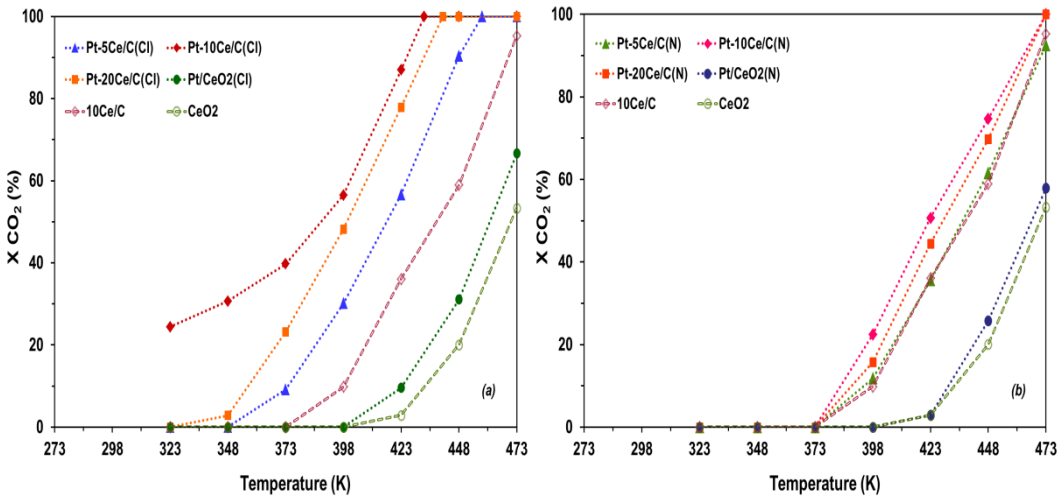

Fig. 5. Yield to CO_2 as a function of reaction temperature for ex-chloride (a) and ex-nitrate (b) catalysts.

Table 1. Textural properties of the supports

Sample	S_{BET} ($m^2 \cdot g^{-1}$)	V_0 ($cm^3 \cdot g^{-1}$)	V_{meso} ($cm^3 \cdot g^{-1}$)
AC	1525	0.51	0.65
5Ce/C	1428	0.48	0.59
10Ce/C	1324	0.45	0.53
20Ce/C	1126	0.40	0.45
CeO_2	124	0.01	0.05

Table 2. Chemical analysis and CeO_2 crystallite size in catalysts

Catalyst	(wt.%)			D (nm)	
	Pt(Cl)	Pt(N)	CeO_2	CeO_2(Cl)	CeO_2(N)
Pt-5Ce/C	0.82	0.75	3.97	5.1	5.9
Pt-10Ce/C	0.89	0.89	7.28	4.8	5.9
Pt-20Ce/C	0.85	0.73	13.18	5.1	5.6
Pt/CeO_2	1.09	0.66		13.7	13.7

Table 3. Pt-10Ce/C(Cl) and Pt-10Ce/C(N) catalysts characterization by XPS

Catalyst	T Red (K)	BE Pt $4f_{7/2}$ (eV)	Pt/Ce	Ce/C	Cl/Ce	Ce^{3+} (%)
Pt-10Ce/C(Cl)	-	72.6 (64.6%); 73.9	0.06	0.01	0.3	43.3
	473	71.5 (54.2%); 73.3	0.04	0.01	0.5	51.3
Pt-10Ce/C(N)	-	71.8 (33.3%); 72.9	0.04	0.03	-	40.4
	473	71.8 (73.5%); 72.9	0.01	0.03	-	42.3

Table 4. Catalytic activity for toluene hydrogenation at 333 K for catalyst reduced at 473 and at 773 K.

Catalyst	Activity (μmol MCH·s^{-1}·gPt^{-1})	
	Red 473 K	**Red 773 K**
Pt-5Ce/C(Cl)	30.93	0.58
Pt-5Ce/C(N)	16.91	0.14
Pt-10Ce/C(Cl)	137.80	0.29
Pt-10Ce/C(N)	12.94	2.25
Pt-20Ce/C(Cl)	24.32	0.47
Pt-20Ce/C(N)	11.96	2.41
Pt/CeO_2(Cl)	10.59	0.12
Pt/CeO_2(N)	6.09	0.10